Vol. 14, No. 1: 1-10
December 2025
DOI: https://10.22487/25411969.2025.v14.i1.17649

Natural Science
Journal of Science and Technology

Original article

In Silico Evaluation of Cardamom Compounds Against DNA Gyrase and NADPH Oxidase

Sri Ainun[1], Try Novika[1], Indriani[1], Nov Irmawati Inda[1], Pasjan Satrimafitrah[*1,2]

[1]*Department of Chemistry, Faculty of Mathematics and Natural Sciences, Tadulako University, Jl. Soekarno Hatta Km. 9, Palu, 94148, Indonesia*
[2]*Department of Postgraduate Chemistry, Faculty of Mathematics and Natural Sciences, Tadulako University, Jl. Soekarno Hatta Km. 9, Palu, 94148, Indonesia*

Keywords: *Amomum compactum, molecular docking, ADMET analysis, natural drug discovery, pharmacokinetics.*

Article history:
Received : 07 February 2025
Accepted : 19 September 2025
Published : 25 December 2025

**Coresponding Author:*
pasjan@untad.ac.id

Abstract

This study evaluates bioactive compounds from local cardamom (*Amomum compactum*) as possible antibacterial and antioxidant lead molecules using molecular docking and in-silico ADMET prediction. DNA gyrase (PDB ID: 6F86) and NADPH oxidase (PDB ID: 2CDU) were selected as targets for antibacterial and antioxidant activity, respectively. Twenty-six candidate compounds were screened; the ten top-ranked compounds (by combined docking score and ADMET profile) were analyzed further. Docking identified β-sesquiphellandrene, 1-piperoylpiperidine, 1,8-cineole, and α-terpineol as showing favorable binding modes. In silico ADMET (pkCSM) showed that 1,8-cineole and α-terpineol satisfy common oral bioavailability and safety criteria. Docking validations (redocking co-crystallized ligands) yielded RMSD = 1.414 Å for 6F86 and RMSD = 1.554 Å for 2CDU. Taken together, these in silico results support targeted in vitro validation for the most promising compounds.

INTRODUCTION

Infectious diseases caused by pathogenic bacteria remain a global health problem. One way of dealing with them is with antibiotics, but antibiotic resistance continues to increase, making them less effective (Neubeiser *et al*., 2020). Based on Global Research on Antimicrobial Resistance data in 2022, bacterial resistance is the world's second-largest cause of death (Murray *et al*., 2022). Therefore, new antibiotics are needed, including those sourced from nature.

Natural products are often considered safer due to their plant-based origins. One such plant with significant antibacterial potential is cardamom (*Amomum compactum*), a member of the Zingiberaceae family. Traditionally, cardamom has been used to treat various ailments, including sore throat (Silalahi, 2017). Research indicates that ethanol extract from cardamom seeds can inhibit the growth of *Streptococcus pyogenes*, the bacterium responsible for pharyngitis. These findings suggest that cardamom holds promise as a potential candidate for treating bacterial infections (Komala *et al*., 2020). Additionally, cardamom contains bioactive compounds such as phenolic compounds, flavonoids, volatile oils, and minerals, which exhibit antioxidant and anti-inflammatory properties (Winarsi *et al*., 2013).

How to Cite: Ainun, *et al*. "In Silico Evaluation of Cardamom Compounds Against DNA Gyrase and NADPH Oxidase" Natural Science: Journal of Science and Technology. Vol. 14, No. 1: 1–10, December 2025.

Given these diverse biological activities, cardamom has attracted growing interest as a source of multifunctional therapeutic agents. However, identifying which specific compounds contribute to its antibacterial and antioxidant effects requires systematic molecular investigation.

One effective method for studying the interaction of specific compounds is through *in silico* molecular approaches, such as molecular docking. This technique is widely used in drug design to identify interactions between compounds and target proteins rapidly and cost-effectively (Tumilaar *et al*., 2021). Molecular docking predicts the binding affinity and stability of compounds by analyzing interactions such as hydrogen bonds, hydrophobic interactions, and Van der Waals forces. These interactions are critical in determining the potential efficacy of a compound as a drug candidate (Hasnaa *et al*., 2022). Tools like PyRx are commonly employed to perform docking simulations and analyze these molecular interactions, while ADMET analysis helps ensure the safety and effectiveness of compounds.

Integrating molecular docking with ADMET prediction allows researchers to not only identify promising bioactive molecules but also assess their drug-likeness early in the discovery process, thereby strengthening the rationale for further experimental testing (Bultum *et al*., 2022).

DNA gyrase is an attractive target for designing new antibacterial drugs because it plays an important role in DNA replication, transcriptional recombination repair, and chromosome decompression. Inhibiting this enzyme will lead to cell death (Khan *et al*., 2018). Thus, blocking DNA gyrase activity represents a well-established strategy for suppressing bacterial proliferation. Meanwhile NADPH oxidase is an enzyme that produces reactive oxygen species (ROS), which contribute to tissue damage in various diseases. (Cipriano *et al*., 2023). Because excessive ROS leads to oxidative stress, inhibiting NADPH oxidase may help reduce inflammation and oxidative injury.

Local Cardamom (*Amomum compactum*) contains chemical compounds that potentially interact with DNA gyrase and NADPH oxidase. However, the mechanism of action of compounds derived from cardamon against DNA gyrase and NADPH Oxidase remain unclear. Therefore, a systematic in silico assessment is needed to clarify how cardamom-derived compounds may modulate these molecular targets and to identify which constituents offer the most promising therapeutic potential. This study was aimed to evaluate compounds in local Cardamom using molecular docking method and ADMET analysis. The research focused on the ability of these compounds to interact with DNA gyrase and NADPH oxidase as molecular targets, that is expected to generate effective natural drug candidates to address bacterial infections and ROS-related diseases.

Material and Methods

Exploration of compounds contained in cardamom *(Amomum compactum)*

The secondary metabolites of cardamom plants were retrieved from Dr. Dukes Phytochemical and Ethnobotanical database and literature search (Yasmin *et al*., 2022). 26 compounds were selected for analysis. Furthermore, the ligand files (sdf format) were downloaded from the PubChem website (https://pubchem.ncbi.nlm.nih.gov/).

ADMET Prediction

ADMET properties were predicted using online tools by inputting selected ligand SMILES codes and evaluating bioavailability, metabolism, and toxicity parameters. (Yeni *et al*., 2018). For each ligand, SMILES strings were submitted to the pkCSM web server (https://biosig.lab.uq.edu.au/pkcsm/) to predict absorption, distribution, metabolism, excretion and toxicity endpoints. We report Lipinski rule of five metrics (molecular weight, LogP, H-bond acceptors and donors) and pkCSM outputs: Caco-2 permeability (log Papp, $\times 10^{-6}$ cm/s), intestinal absorption (%), P-glycoprotein substrate/inhibitor status, volume of distribution (VDss, log L/kg), blood–brain barrier permeability (LogBB), CYP450 substrate/inhibitor predictions (CYP1A2, CYP2C9, CYP2C19, CYP2D6, CYP3A4), total clearance (log ml/min/kg), renal OCT2 substrate status, AMES toxicity, maximum tolerated dose (log mg/kg/day), hERG I/II inhibition, and hepatotoxicity. Thresholds used for positive selection were: intestinal absorption >30%, Caco-2 log Papp > 0.9, AMES = negative, and no predicted hERG I inhibition. Results are provided in Table 1 (ADMET).

Molecular Docking

Protein structures were downloaded from the RCSB Protein Data Bank (DNA gyrase, PDB ID: 6F86; NADPH oxidase, PDB ID: 2CDU) as seen in Figure 1. Receptor preparation used AutoDockTools/MGLTools to remove water molecules and non-essential heteroatoms, add polar hydrogens, and assign Gasteiger charges; prepared macromolecules were saved in PDBQT format (Prasetio *et al*., 2021). Ligand structures (SDF from PubChem) were converted to PDBQT using OpenBabel 2.4.1. after energy minimization with the MMFF94 force field. Docking runs were performed

using AutoDock Vina (via PyRx – Python Prescription 0.8) (Ruswanto *et al*., 2018). Vina settings: exhaustiveness = 8, number of output modes = 9, energy_range = 3.0 kcal·mol^{-1}. Grid box sizes used in PyRx: for 6F86 — x = 62.3158 Å, y = 28.0540 Å, z = 64.8347 Å; for 2CDU — x = 15.287 Å, y = 13.8698 Å, z = 20.3464 Å (these are the box sizes used in the PyRx project file). Binding poses were visualized in Discovery Studio Visualizer 2021 Client and PyMOL 2.4.1; key interactions were recorded and distances reported in Å. (Dassault System, 2009). Method validation was performed using PyMol to find the root mean square deviation (RMSD) value (Syaqila *et a*l., 2024).

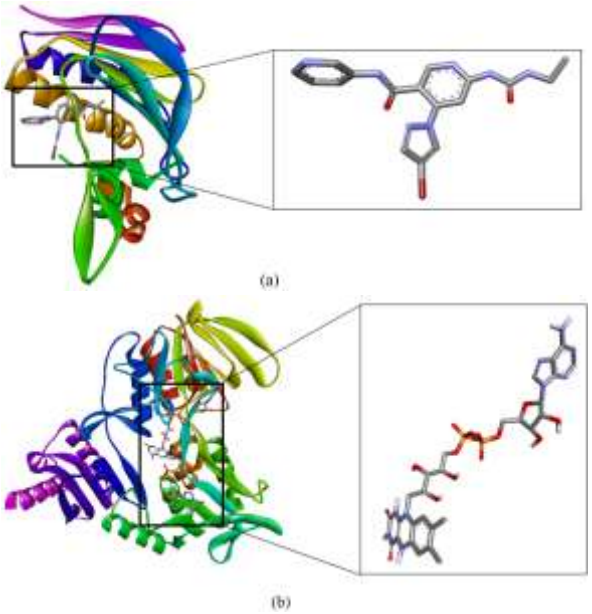

Fig 1. 3D structure of DNA gyrase and *4-(4-bromanylpyrazol-1-yl)-6-(ethylcarbamoylamino)-~{N}-pyridin-3-yl-pyridine-3 carboxamide* (native ligand) (a), 3D structure of NADPH Oxidase and *flavin-adenine dinucleotide (*native ligand) (b).

Results and Discussion

ADMET analysis

The calculation of ADMET properties is shown in Table 1. Four properties are calculated in the Lipinski rule, and the 10 best ligands out of 26 test ligands meet all the threshold parameters, indicating that all ligands have good solubility and permeability in the human body. Other properties, such as distribution, metabolism, excretion, and toxicity of each ligand, showed that the 10 best ligands fulfill all parameters. In adsorption parameters, a compound is considered to have a high $CaCO_2$ permeability (greater than 0.9), high intestinal absorption (> 30%), and not act as the substrate and inhibitor of P-glycoprotein. By these threshold parameters, it can be shown that only 1,8-*cineole*, *cis-sabinene hydrate*, *alpha-terpineol*, *beta-bisabolene*, i, *alpha-pinene, carvone*, and *terpinen*-4-*ol*.

In distribution parameters, the compounds should have a low volume of distribution (VDss) (< -0.15) and a blood-brain barrier (BBB) higher than 0.3, and it is shown that all ligands fulfill these parameters. In metabolism parameters, a compound is considered a cytochrome P450 inhibitor by inhibiting CYP2D6 or CYP3A4 substrate. The calculation results show that all the compounds are not substrates or inhibitors of CYP2D6, CYP3A4, CYP1A2, and CYP2C19. In excretion parameters, all compounds did not act as renal OCT2 substrates. AMES toxicity assesses the mutagenic properties of the compound in bacteria, and all compounds show nontoxic properties.

Docking Method Validation

We validated the docking protocol by redocking co-crystallized ligands into their receptors using the same preparation and Vina settings. RMSD between the redocked and crystallographic poses was calculated in PyMOL. The RMSD values were 1.414 Å for the 6F86 native ligand and 1.554 Å for the 2CDU native ligand, both below the commonly accepted 2.0 Å threshold, indicating the docking protocol reproduced native ligand geometries adequately (Wahyuni *et al*. 2022). Native ligands' Vina binding energies (computed during redocking) are reported in Table 2 for comparison.

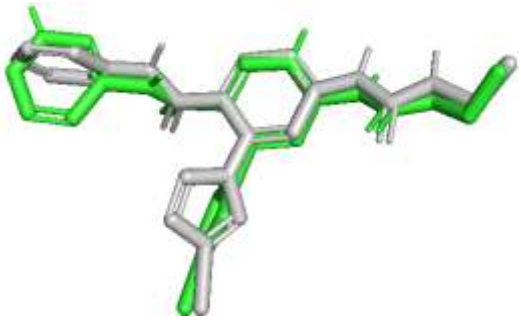

Fig 2. Validation of the 4-(4-bromanylpyrazol-1-yl)-6-(ethylcarbamoylamino)-~{N}-pyridin-3-yl-pyridine-3 carboxamide (native ligand) DNA Gyrase (PDB ID: 6F86) before docking (gray) and after redocking (green).

Fig 3. Validation of the flavin-adenine dinucleotide (native ligand) NADPH Oxidase (PDB ID: 2CDU) before docking (gray) and after redocking (blue).

Table 1. Result of ADMET Calculation Properties

	Properties	Ligand*									
		1	**2**	**3**	**4**	**5**	**6**	**7**	**8**	**9**	**10**
Lipinski rule	**Molecular weight (≤ 500)**	154.253	154.253	154.253	204.357	222.372	136.238	150.221	154.253	136.238	154.253
	Log P (≤ 5)	2.7441	2.1935	2.5037	5.0354	3.4657	2.9987	2.4879	2.6478	3.3089	2.5037
	Acceptors H-Bond (≤ 10)	1	1	1	0	1	0	1	1	0	1
	Donors H-Bond (≤ 5)	0	1	1	0	1	0	0	1	0	1
Absorption	**$CaCO_2$ Permeability (log Papp in 10^{-6} cm/s)**	**1.485**	1.494	1.489	1.429	1.483	1.38	1.413	1.49	1.401	1.502
	Intestinal absropsi (% absorbed)	**96.505**	94.786	94.183	95.232	92.814	96.041	97.702	93.426	95.898	94.014
	P-glycoprotein substrate (Yes/No)	No	No	No	No	No	No	No	Yes	Yes	No
	P-glycoprotein I inhibitor (Yes/No)	No	No	No	No	No	No	No	No	No	No
	P-glycoprotein II inhibitor (Yes/No)	**No**	No	No	No	No	No	No	No	No	No
Distribution	**VDss (Log L/kg)**	0.491	0.351	0.207	0.634	0.556	0.667	0.179	0.189	0.396	0.21
	BBB permeability (Log BB)	0.368	0.663	0.305	0.788	0.632	0.791	0.588	0.3	0.732	0.563
Metabolism	**CYP2D6 substrate (Yes/No)**	No	No	No	No	No	No	No	No	No	No
	CYP3A4 substrate (Yes/No)	No	No	No	No	Yes	No	No	No	No	No
	CYP1A2 inhibitor (Yes/No)	No	No	No	No	Yes	No	No	No	No	No
	CYP2C19 inhibitor (Yes/No)	No	No	No	No	No	No	No	No	No	No
	CYP2C9 inhibitor (Yes/No)	No	No	No	No	No	No	No	No	No	No
	CYP2D6 inhibitor (Yes/No)	No	No	No	No	No	No	No	No	No	No
	CYP3A4 inhibitor (Yes/No)	No	No	No	No	No	No	No	No	No	No
Excretion	**Total Clearance (Log ml/min/kg)**	1.009	1.001	1.219	1.458	0.817	0.043	0.225	1.222	0.213	1.269
	Renal OCT2 Substrate (Yes/No)	No	No	No	No	No	No	No	No	No	No
Toxicity	**AMES Toxicity (yes/No)**	No	No	No	No	No	No	No	No	No	No
	Max. Tolerated dose (Log mg/kg/day)	0.553	0.637	0.886	0.418	-0.193	0.48	0.775	0.861	0.777	0.857
	HerG I inhibitor (Yes/No)	No	No	No	No	No	No	No	No	No	No

HerG II inhibitor (Yes/No)	No	No	No	No	No	No	No	No	No	No
Hepatoxicity (Yes/No)	No	No	No	No	No	No	No	No	No	No
Skin Sensitisation (Yes/No)	Yes	Yes	Yes	Yes	Yes	No	Yes	Yes	Yes	Yes
T.Pyriformis toxicity (Log ug/L)	0.171	0.323	0.008	1.943	1.369	0.45	0.41	-0.019	0.579	0.189
Minnow toxicity Log mM)	1.735	1.337	1.8	-0.065	1.063	1.159	1.445	1.871	1.203	1.545

***ligands:** 1. 1,8-cineole; 2, cis-sabinene hydrate; 3. alpha-terpineol; 4. beta-bisabolene; 5. d-ledol; 6. alpha-pinene; 7. Carvone; 8. Gamma-terpineol; 9. Limonene; 10. terpinene-4-ol.

Table 2. RMSD and binding energy of docking validation of native ligands and receptors

Receptors	Native Ligands	RMSD	Binding energy (kcal/mol)
DNA Gyrase (PDB 6F86)	4-(4-bromanylpyrazol-1-yl)-6-(ethylcarbamoylamino)-~{N}-pyridin-3-yl-pyridine-3-carboxamide	1.414 Å	-8.1
NADPH Oxidase (PDB 2CDU)	flavin-adenine dinucleotide	1.554 Å	-11.7

Molecular Docking Analysis

Molecular docking was performed on the 10 best ligand targets with DNA Gyrase (PDB code: 6F86) and NADPH Oxidase (PDB code: 2CDU) as target proteins. Molecular docking analysis was observed by the binding energy (ΔG) and the binding interaction between the ligand and the target receptor as seen in Table 3.

Table 3. Docking result of selected compounds with receptors DNA gyrase and NADPH Oxidase

		DNA gyrase				NADPH Oxidase			
No	Ligand	Binding Affinity (kkal/mol)	Residues	Interactions	Distance (Å)	Binding Affinity (kkal/mol)	Residues	Interactions	Distance (Å)
1	*Native ligand*	-8.1	**ASN 46**,	Hydrogen bond	2.76	-11.7	ALA 11	Hydrogen bond	1.87
			ARG 136,	Hydrogen bond	3.03		THR 301	Hydrogen bond	2.60
			ASP 73,	Hydrogen bond	2.79		PRO 298	Hydrogen bond	3.59
			GLY 77,	Hydrogen bond	2.75		ASP 282	Hydrogen bond	2.67
			PRO 79,	Hydrogen bond	3.35		**HIS 10**	Hydrogen bond	1.87; 2.38
			VAL 43	Hydrogen bond	3.71		GLY 114	Hydrogen bond	3.22
			ILE 94,	Hydrofobic bond	4.28; 4.86		SER 115	Hydrogen bond	2.09; 2.90
			VAL 71,	Hydrofobic bond	4.32		THR 9	Hydrogen bond	1.92
			VAL 167	Hydrofobic bond	4.54		MET 33	Hydrogen bond	2.48; 3.83; 3.73
			ILE 78,	Hydrofobic bond	4.85; 4.83		HIS 79	Hydrogen bond	3.37
			ARG 76	Hydrofobic bond	4.90		VAL 81	Hydrogen bond	1.99; 2.07
							GLU 32	Hydrogen bond	3.88; 2.46
							THR 113	Hydrogen bond	3.82
							LEU 299	Hydrofobic bond	5.16

							ALA 300	Hydrofobic bond	4.55
							LYS 134	Hydrofobic bond	3.26
							VAL 6	Hydrofobic bond	3.83
							ILE 160	Hydrofobic bond	3.71
							CSX 42	Unfavorable acceptor-acceptor	1.43
2	*Ciprofloxacin*	-6.2	**ASP 73**	Halogen bond	3.21				
			ASN 46,	Hydrophobic bond	5.35				
			GLY 77,	Hydrophobic bond	5.44				
			ILE 94,	Hydrophobic bond	4.34				
			ILE 78	Hydrophobic bond	4.59; 4.54				
3.	Vitamin C					-6.3	THR 112	Hydrogen bond	1.88
							GLY 12	Hydrogen bond	2.28
							ASP 282	Hydrogen bond	2.05
							HIS 10	Hydrogen bond	2.08
							THR 9	Hydrogen bond	2.52
							SER 115	Unfavorable donor-donor	2.04
							LYS 134	Hydrogen bond	2.26
4.	*1,8-Cineole*	-4.5	ILE 78	Hydrophobic bond	5.00	-5.4	ALA 300	Hydrofobic bond	4.36
							ALA 303	Hydrofobic bond	4.18
							HIS 10	Hydrofobic bond	5.46; 5.42
							THR 9	Hydrogen bond	2.53
5.	*Cis-Sabinene hydrate*	-5.1	**ASN 46**	Hydrogen bond	2.00	-5.4	ALA 303	Hydrophobic bond	4.18
							ALA 300	Hydrophobic bond	4.36
							HIS 10	Unfavorable acceptor-acceptor	3.76; 5.03
							ASP 282	Unfavorable acceptor-acceptor	2.97
6.	*Alpha-terpineol*					-6.0	**HIS 10**	Hydrogen bond	2.77
							ALA 300	Hydrofobic bond	3.96
							ALA 303	Hydrofobic bond	4.13
7.	*Beta-Bisabolene*	-6.1	ILE 71	Hydrophobic bond	4.53	-6.5	ALA 303	Hydrofobic bond	3.83
			ALA 47	Hydrophobic bond	4.22;5.34		**ALA 300**	Hydrofobic bond	4.44
			ILE 78	Hydrophobic bond	5.05;5.21		PHE 245	Hydrofobic bond	5.23
			VAL I67	Hydrophobic bond	4.80		ILE 160	Hydrofobic bond	3.83; 4.34
			VAL 43	Hydrophobic bond	4.81		ILE 44	Hydrofobic bond	4.05
			ILE 94	Hydrophobic bond	5.24;4.24		CYS 133	Hydrofobic bond	4.54
8.	*Beta-Sesquiphellandrene*	-6.5	ALA 47	Hydrophobic bond	4.96	-6.4	PHE 245	Hydrofobic bond	4.10

			VAL 71	Hydrophobic bond	4.55		LYS 134	Hydrofobic bond	4.59
			VAL 167	Hydrophobic bond	4.30		**ALA 300**	Hydrofobic bond	4.19
			VAL 43	Hydrophobic bond	4.94		**ALA 11**	Hydrofobic bond	5.08; 4.06
			ILE 78	Hydrophobic bond	5.25; 4.84		ALA 303	Hydrofobic bond	5.03; 4.31
			PRO 79	Hydrophobic bond	4.57		HIS 10	Unfavorable bump	2.19
			ILE 94	Hydrophobic bond	4.67				
9.	*d-Ledol*	-6.1	ILE 78	Hydrophobic bond	4.97	-7.1	ALA 11	Hydrogen bond	2.04
			PRO 79	Hydrophobic bond	5.27		ALA 303	Hydrofobic bond	4.97
			THR 165:	Unfavorable Acceptor-Acceptor:	1.65				
10.	*1-Piperoylpiperidine*	-6.3	**ASN 46**	Hydrogen bond	1.90;3.89	-8.9	Val 81	Hydrogen bond	3.18; 2.14
			GLY 77	Hydrogen bond	3.38		MET 33	Hydrofobic bond	3.71
			ALA 47,	Hydrophobic bond	5.44		ALA 303	Hydrofobic bond	4.62
			ILE 78,	Hydrophobic bond	4.95		ALA 11	Hydrofobic bond	5.25
			PRO 79	Hydrophobic bond	4.60				
11.	*Carvone*	-5.5	**GLY 77**	Hydrogen bond	2.73	-6.0	ALA 11	Hydrogen bond	2.12
			ALA 47	Hydrofobic bond	4.96		ALA 303	Hydrofobic bond	4.05
			ILE 78,	Hydrofobic bond	5.04; 5.27		**ALA 300**	Hydrofobic bond	4.92; 3.77
			VAL 167	Hydrofobic bond	5.07		**HIS 10**	Unfavorable bump	2.13; 5.29
12	*Gamma-Terpineol*	-5.2	GLU 50	Hydrogen bond	4.93	-5.5	ASP 282	Hydrogen bond	2.93
			ILE 78	Hydrofobic bond	4.93		ALA 11	Hydrofobic bond	3.77
13	*Limonene*	-5.1	ILE 78	Hydrofobic bond	4.74	-5.3	ILE 44	Hydrofobic bond	4.02
							PHE 245	Hydrofobic bond	3.74
							ILE 160	Hydrofobic bond	4.49; 383
							CYS 133	Hydrofobic bond	4.45
14	*Terpinen-4- OL*	-5.1	ILE 78	Hydrofobic bond	4.60; 5.37	-5.6	LYS 134	Hydrogen bond	1.88; 4.78
			ASN 46	Hydrogen bond	3.04		LYS 134	Hydrogen bond	2.26

*Amino acid residues given in bold are active sites (Narramore *et al*., 2019; Lountos *et al*., 2006)

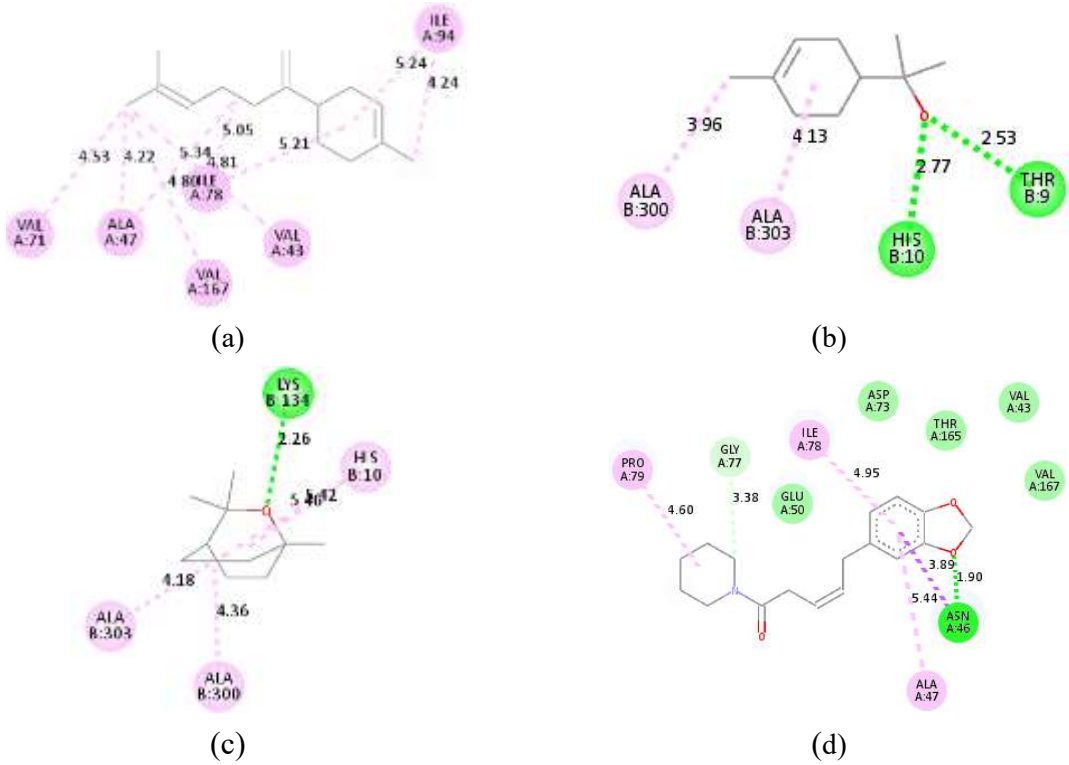

Fig 4. Interaction between beta-sesquiphellandrene (a) and 1-piperoylpiperidine (b) on binding site of DNA gyrase; 1,8-cineole (c) and 1,8- alpha-terpineol (d) on binding site of NADPH oxidase

The standard ligand used in this study is ciprofloxacin, a DNA gyrase inhibitor used as an antibacterial drug, and vitamin C, an antioxidant that attenuates NADPH Oxidase. The value of the bond energy formed is a calculation of the conformation of the ligand formed in a macromolecule (Susanti et al., 2019). As a ligand-receptor in the lowest energy condition, the molecule will be in a stable condition, thus the ΔG getting lower (Suhadi *et al*., 2021).

Based on molecular docking results in DNA Gyrase receptor, cardamom compounds still have higher binding energy than standard ligands (ciprofloxacin). Still, two compounds (beta-sesquiphellandrene and 1-piperoylpiperidine) have the lowest binding energy among other compounds and can be used as new inhibitors. The results of NADPH Oxidase showed that cardamom compounds have higher binding energy than the standard ligand (Vitamin C). Specifically, 1,8-cineole and alpha-terpineol exhibited higher binding energy than the standard ligand.

Furthermore, visualization observations were carried out, as shown in Figure 4, to determine the amino acids that play a role in inhibiting the DNA gyrase and NADPH Oxidase. The result of these visualization observations is the interaction of amino acid residues with ligands. The amino acid interactions involved allow contact between the ligand and the receptor so that it has inhibitory activity. (Sari *et al*., 2020).

Beta-sesquiphellandrene has amino acid residues in common with the DNA gyrase receptor, namely PRO 79 and ILE 94 in the hydrophobic bond, while 1-piperoylpiperidine shows the similarity of binding positions of amino acid residues through hydrogen bonds and Van Der Waals interaction bonds, namely Asn 46, Gly 77 and PRO 79. 1.8-cineole has amino acid residues in common with the NADPH Oxidase receptor on hydrophobic bonds, namely HIS 10 and ALA 300. In comparison, alpha-terpineol shows the similarity of binding positions of amino acid residues through hydrogen bonds and Van Der Waals interaction (hydrophobic bond), namely HIS 10 and ALA 300.

CONCLUSION

In silico docking and ADMET screening identified several Amomum compactum metabolites — notably 1,8-cineole and α-terpineol — as promising candidates for further antibacterial and antioxidant study. Because docking and in silico ADMET are predictive, we recommend prioritized in vitro follow-up: (i) MIC assays against representative bacteria (including Streptococcus pyogenes), (ii) DNA gyrase inhibition assays for hits targeting gyrase, (iii) NADPH oxidase activity / ROS assays for antioxidant candidate validation, and (iv) cytotoxicity testing on

mammalian cell lines. These steps will establish whether the in silico predictions translate into biological activity.

REFERENCES

Cipriano, A., Viviano, M., Feoli, A., Milite, C., Sarno, G., Castellano, S., & Sbardella, G. 2023. NADPH oxidases: from molecular mechanisms to current inhibitors. Journal of medicinal chemistry. *66*(17), 11632-11655. https://doi.org/10.1021/acs.jmedchem.3c00770.

Dassault system. 2019. *Biovia Discovery Studio Visualizer*. Dassault Systems.

Hasnaa, N. R., & Manalu, R. T. 2022. Molecular Docking of Turmeric Active Compounds (Curcuma longa L.) against Main Protease in Covid-19 Disease. East Asian Journal of Multidisciplinary Research. 1(3), 353-364. https://doi.org/10.55927/eajmr.v1i3.101.

Khan, T., Sankhe, K., Suvarna, V., Sherje, A., Patel, K., & Dravyakar, B. 2018. DNA gyrase inhibitors: Progress and synthesis of potent compounds as antibacterial agents. Biomedicine & Pharmacotherapy. *103*, 923-938. https://doi.org/10.1016/j.biopha.2018.04.021.

Komala, O., Ismanto, Maulana, M.A. 2020. Aktivitas Antibakteri Ekstak Etanol Biji Kapulaga Jawa (Amomum Compactum Soland. Ex Maton) Terhadap Streptococcus pyogenes. Ekologi: Jurnal Ilmiah Ilmu Dasar dan Lingkungan Hidup. 20(1): 31-39. https://doi.org/10.33751/ekologia.v20i1.1985.

Lountos, G. T., Jiang, R., Wellborn, W. B., Thaler, T. L., Bommarius, A. S., & Orville, A. M. 2006. The crystal structure of NAD (P) H oxidase from Lactobacillus sanfranciscensis: insights into the conversion of O_2 into two water molecules by the flavoenzyme. Biochemistry. 45(32), 9648-9659. https://doi.org/10.1021/bi060692p.

Murray, C. J., Ikuta, K. S., Sharara, F., Swetschinski, L., Aguilar, G. R., Gray, A., ... & Tasak, N. 2022. Global burden of bacterial antimicrobial resistance in 2019: a systematic analysis. The lancet. *399*(10325), 629-655.

Narramore, S., Stevenson, C. E., Maxwell, A., Lawson, D. M., & Fishwick, C. W. 2019. New insights into the binding mode of pyridine-3-carboxamide inhibitors of E. coli DNA gyrase. Bioorganic & medicinal chemistry. *27*(16), 3546-3550. https://doi.org/10.1016/j.bmc.2019.06.015.

Neubeiser, A., Bonsignore, M., Tafelski, S., Alefelder, C., Schwegmann, K., Rüden, H., ... & Nachtigall, I. 2020. Mortality attributable to hospital acquired infections with multidrug-resistant bacteria in a large group of German hospitals. Journal of infection and public health. 13(2), 204-210. https://doi.org/10.1016/j.jiph.2019.07.025.

Perdana, A. T., & Permana, A. A. 2021. Molecular Docking Senyawa Potensial Anticovid-19 Secara In Silico. JIKA (Jurnal Informatika). 5(2): 159-166. http://dx.doi.org/10.31000/jika.v5i2.4516.

Prasetio, N.F., Kepel, B.J., Bodhi, W., dan Fatimawali. 2021. Molecular Docking terhadap Senyawa Isoleutherin dan Isoeleutherol sebagai Penghambat Pertumbuhan SARS-CoV-2. e-Biomedik. . 9(1): 101-106. https://doi.org/10.35790/ebm.v9i1.31809.

Ruswanto, R., Nofianti, T., Mardianingrum, R., & Lestari, T. 2018. Desain dan Studi in silico Senyawa Turunan Kuwanon-H sebagai Kandidat Obat Anti-HIV. Jurnal Kimia VALENSI. .4(1): 57-66. http://dx.doi.org/10.15408/jkv.v4i1.6867.

Sari, I.W., Junaidin, and Pratiwi, D. 2020. Studi Molecular Docking Senyawa Flavonoid Herba Kumis Kucing (*Orthosiphon stamineus B.*) pada Reseptor alpha-glukosidase sebagai Antidiabetes Tipe 2. Jurnal Farmagazine. 7(2), 54-60. http://dx.doi.org/10.47653/farm.v7i2.194.

Silalahi, M. 2017. Bioaktivitas Amomum Compactum Soland Ex Maton dan perspektif konservasinya. Jurnal Pro-Life. 4(2), 320-328. https://doi.org/10.33541/pro-life.v4i2.371.

Suhadi, A., Rizarullah, R., & Feriyani, F. 2019. Simulasi docking senyawa aktif daun binahong sebagai inhibitor enzyme aldose reductase. Sel Jurnal Penelitian Kesehatan. *6*(2), 55-65. https://doi.org/10.22435/sel.v6i2.1651.

Susanti, N.M.P., Laksimiani, N.P.L., Noviyanti, N.KM., Arianti, K.M., dan Duantara, I.K. 2019. Molecular Docking Terpinen-4-ol sebagai Antiinflamasi pada Aterosklerosis secara *In Silico*. Jurnal Kimia. 13(2), 221-228. https://doi.org/10.24843/JCHEM.2019.v13.i02.p16.

Syaqila, C. N., Pebralia, J., & Restianingsih, T. 2024. Molecular Docking Senyawa (8)-Shogaol Sebagai Obat Antikanker. Journal Online Of

Physics. *9*(3), 72-76. https://doi.org/10.22437/jop.v9i3.36116.

Tumilaar, S. G., Siampa, J. P., & Tallei, T. E. 2021. Penambatan Molekuler Senyawa Bioaktif dan ekstrak Etanol Daun Pangi (*Pangium edule*) Terhadap Reseptor Protease HIV-1, Jurnal Ilmiah Sains. 21(1), 6. https://doi.org/10.35799/jis.21.1.2021.30282.

Wahyuni, W., Diniantini, A., Ghozali, M., & I, S. 2022. Etlingera Genus: Phytochemical Screening and Anticancer Activity. Jurnal Farmasi Sains dan Praktis. 7(3), 136-149. https://doi.org/10.31603/pharmacy.v7i3.6120.

Winarsi, H., Sasongko, N. D., Purwanto, A., & Nuraeni, I. 2013. Ekstrak daun kapulaga menurunkan indeks atherogenik dan kadar gula darah tikus diabetes induksi alloxan. Agritech. *33*(3), 273-280. https://doi.org/10.22146/agritech.9548.

Yasmin, R., Mafiroh W.U., Kinasih, A., Ramadhani, A.N., Putri, R., Semiarti, E. 2022. Potential of Anti-Cancer and Antimicrobial in Orchid Based on Prediction of Activity Spectra for Substances (Pass) Online. Journal of Agromedicine and Medical Sciences. 8(1), 25-23. https://doi.org/10.19184/ams.v8i1.2684 8

Yeni, Supardi, Fajar Merdekawati 2018. In silico toxicity prediction of 1-phenyl-1-(qunazolin-4-yl) ethanol compunds by using Toxtree, pkCSM and preADMET. Pharmaciana. 8(2): 205-216. https://doi.org/10.12928/pharmaciana.v8i2.9508

.